The FEBS Journal

FEBS PRESS science publishing by scientists

Regulating levels of the neuromodulator D-serine in human brain: structural insight into pLG72 and D-amino acid oxidase interaction

Leila Birolo[1], Silvia Sacchi[2,3], Giovanni Smaldone[4], Gianluca Molla[2,3], Gabriella Leo[1], Laura Caldinelli[2,3], Luciano Pirone[5], Patrick Eliometri[2], Sonia Di Gaetano[5], Ida Orefice[1], Emilia Pedone[5], Piero Pucci[1] and Loredano Pollegioni[2,3]

1 Dipartimento di Scienze Chimiche, Università degli Studi di Napoli Federico II, Napoli, Italy
2 Dipartimento di Biotecnologie e Scienze della Vita, Università degli studi dell'Insubria, Varese, Italy
3 Centro Interuniversitario di Ricerca in Biotecnologie Proteiche "The Protein Factory", Politecnico di Milano and Università degli studi dell'Insubria, Milano, Italy
4 IRCCS SDN, Napoli, Italy
5 Italian Research National Council, Institute of Biostructures and Bioimaging, Napoli, Italy

Keywords
D-amino acid oxidase; D-serine; protein–protein interaction; regulation; schizophrenia

Correspondence
L. Pollegioni, Dipartimento di Biotecnologie e Scienze della Vita, Università degli studi dell'Insubria, via J.H. Dunant 3, 21100 Varese, Italy
Fax: +390332421506
Tel: +390332421500
E-mail: loredano.pollegioni@uninsubria.it

LB and SS equally contributed to this work.

(Received 15 March 2016, revised 28 June 2016, accepted 8 July 2016)

doi:10.1111/febs.13809

The human flavoenzyme D-amino acid oxidase (hDAAO) degrades the NMDA-receptor modulator D-serine in the brain. Although hDAAO has been extensively characterized, little is known about its main modulator pLG72, a small protein encoded by the primate-specific gene *G72* that has been associated with schizophrenia susceptibility. pLG72 interacts with neosynthesized hDAAO, promoting its inactivation and degradation. In this work, we used low-resolution techniques to characterize the surface topology of the hDAAO–pLG72 complex. By using limited proteolysis coupled to mass spectrometry, we could map the exposed regions in the two proteins after complex formation and highlighted an increased sensitivity to proteolysis of hDAAO in complex with pLG72. Cross-linking experiments by using bis(sulfosuccinimidyl)suberate identified the single covalent bond between T182 in hDAAO and K62 in pLG72. In order to validate the designed mode of interaction, three pLG72 variants incrementally truncated at the C terminus, in addition to a form lacking the 71 N-terminal residues, were produced. All variants were dimeric, folded, and interacted with hDAAO. The strongest decrease in affinity for hDAAO (as well as for the hydrophobic drug chlorpromazine) was apparent for the N-terminally deleted pLG72$^{72-153}$ form, which lacked K62. On the other hand, eliminating the disordered C-terminal tail yielded a more stable pLG72 protein, improved the binding to hDAAO, although giving lower enzyme inhibition. Elucidation of the mode of hDAAO–pLG72 interaction now makes it possible to design novel molecules that, by targeting the protein complex, can be therapeutically advantageous for diseases related to impairment in D-serine metabolism.

Abbreviations
BS^3, bis(sulfosuccinimidyl)suberate; CPZ, chlorpromazine; DAAO, D-amino acid oxidase; DTT, dithiothreitol; FAD, flavin adenine dinucleotide; Glu-C, endoprotease Glu-C; hDAAO, human D-amino acid oxidase; NLS, *N*-lauroylsarcosine; NMDAR, *N*-methyl-D-aspartate receptor; RP-HPLC, reverse-phase high-performance liquid chromatography; SPR, surface plasmon resonance; TFA, trifluoroacetic acid.

Introduction

D-Amino acid oxidase (DAAO, EC 1.4.3.3) is a peroxisomal, homodimeric flavoenzyme displaying the properties of the dehydrogenase-oxidase class of flavoproteins. It catalyzes the oxidative deamination of D-amino acids into the corresponding α-keto acids with the concomitant production of ammonia and hydrogen peroxide [1,2]. In the brain, DAAO modulates the concentration of D-serine, an allosteric coactivator of the NMDA type of glutamate receptors (NMDAR), which is mainly produced in neurons through the racemization reaction catalyzed by the enzyme serine racemase [3,4] and is released by neurons and astrocytes [5]. Through the action on NMDAR, the D-serine signaling system plays a key role in developing brain wiring and regulating higher brain functions, including cognitive, emotional, and sensorimotor function [6]. On the other hand, aberrant D-serine-dependent NMDAR activation is involved in a variety of neurological diseases: excessive production/release of D-serine is implicated in acute and chronic degenerative disorders while abnormally low levels have been observed in patients affected by psychiatric disorders such as schizophrenia or bipolar disorders [7–11]. In light of these findings, it was assumed that a possible imbalance in the levels or activities of the enzymes involved in D-serine metabolism might be involved in the onset of such diseases.

We recently demonstrated that the function of human DAAO (hDAAO) is regulated by the interacting protein pLG72: its binding modifies tertiary structure and causes a time-dependent loss of activity of the flavoenzyme, and thus modulates cellular D-serine levels [12–15]. Notably, the *G72* gene encoding for pLG72 is among the most frequently replicated vulnerability genes for schizophrenia and bipolar disorder; for a comprehensive review, see [16,17]. Several genetic studies also found significant evidence for an association between single nucleotide polymorphisms in the *DAAO* gene and schizophrenia [18], although this conclusion is widely debated. pLG72 is a 153-amino acid protein [19] with no recognizable functional motifs; hence, it is valuable for investigating the structural details of its interaction with hDAAO in order to shed light on the molecular mechanisms by which pLG72 finely tunes D-serine levels by modulating flavoenzyme activity. However, characterization of the protein complex by high-resolution techniques constitutes an extremely challenging task as: (a) structural information about pLG72 is lacking, (b) pLG72 is soluble in the presence of mild denaturants only [13,20], and (c) no homologous protein has been structurally characterized so far. For this reason, we decided to employ low-resolution strategies, such as those based on the coupling of classical biochemical approaches (limited proteolysis and chemical cross-linking) with the analytical power of mass spectrometric techniques. Actually, by using different proteases and picking only primary cleavage sites, i.e., those occurring on the intact and native structure, it is possible to get a detailed picture of the exposed protein backbone and to compare the different conformations occurring upon formation of complexes with molecular effectors [21–23]. Furthermore, a cross-linking strategy can capture interactions between flexible regions of proteins in solution by covalently linking amino acid side chains, thus providing information on the regions involved in protein–protein interfaces [24,25].

By using this approach, we characterized the surface topology of the hDAAO–pLG72 complex and defined the conformational changes induced in hDAAO by pLG72 binding. Based on this information, we performed molecular modeling of the pLG72 tertiary structure coupled to hDAAO docking simulations. Finally, deletion variants of pLG72 were prepared to evaluate the inferred mode of interaction. Taken together, this analysis sheds light on the hDAAO–pLG72 complex, opening up the opportunity to design molecules aimed to modulate the cellular concentration of D-serine by acting on the stability/activity of hDAAO through pLG72 binding.

Results

Limited proteolysis studies

In the assumption that the distribution of the preferential proteolytic sites is strictly dependent on the protein conformation, limited proteolysis experiments, causing single cleavage events in the protein structure (primary site) and originating complementary peptide fragments ('complementary proteolysis'), seems well suited to investigate conformational changes in protein structure upon formation of protein complexes [21–23,26]. Based on this approach, very few primary, complementary cleavage sites are detected for highly structured proteins that remain largely undigested, thus providing an instrumental, low-resolution picture of the protein topology. Limited proteolysis experiments have been therefore designed to study the surface topology of hDAAO–pLG72 complex on the grounds that the portions of the protein involved in highly structured regions are located at the intersubunits interface and are thus protected from proteases. Enzymatic hydrolysis was carried out on the single proteins as well as on

the hDAAO–pLG72 complex, incubating with proteases at different enzyme-to-substrate (w/w) ratios, investigating the time course of fragment formation by RP-HPLC, and determining the mass by ESI-MS analysis.

Upon endoprotease Glu-C treatment of hDAAO, only one primary cleavage site was detected, as only two fragments that are 'complementary' were identified: peptides 1–249 and 250–347 (cleavage at E249). Similar limited proteolysis experiments were carried out using subtilisin and chymotrypsin: these proteases cleaved at E249 and at the L189, L194, and L250 sites, respectively (see Table 1). Digestion with trypsin deserves some discussion: it produced a mixture of undigested protein (residues 1–347) and the peptide 1–341 (experimental mass value 38811.6 ± 1.7 Da, theoretical mass value 38811.2 Da), indicating that hDAAO is quickly cleaved at R341 and the C-terminal hexapeptide is removed. The high degree of flexibility and accessibility of the C-terminal region deduced from these data is consistent with its absence in the three-dimensional structure of the protein determined by X-ray analysis [27]. Therefore, in the experiments with trypsin, the truncated form 1–341 was considered as the basic hDAAO molecule on which subsequent hydrolysis occurred yielding peptides 1–191 and 192–341, and indicating that a cleavage site was present at Arg191.

The same experimental strategy was used for pLG72: notably, the optimal enzyme-to-substrate ratio was significantly lower than that used for hDAAO, as could be expected by the inferred high flexibility of pLG72 [20]. With the only exception of cleavage at site W61 by chymotrypsin, all the proteases we used acted on residues belonging to the C-terminal part of this small protein (Table 1). Although the complementary peptides in the digestion of pLG72 with endoprotease Glu-C (Glu-C) and subtilisin were not detected, we can still consider E146 and T150 as primary sites as the cleavages occur at the very C-terminal end of the protein, producing small complementary peptides (encompassing seven and three residues in Glu-C and subtilisin digestion of pLG72, respectively) that are then likely promptly digested. In case they were not the actual primary cleavage site, the shift of a couple of positions (unlikely because no fragment closer to the C terminus was detected) does not change dramatically the low-resolution picture of the superficial topology of the protein.

In order to ensure that all the molecules of the flavoenzyme were complexed with pLG72, experiments on the hDAAO–pLG72 complex were carried out using a fivefold molar excess of pLG72 protein (by mixing 4 nmol hDAAO and 20 nmol of pLG72); complex formation was confirmed by native gel analysis (not shown). The large excess of pLG72 hampered to deduce any structural information about the pLG72 regions involved in the complex because most of the pLG72 molecules were not complexed with hDAAO. As far as hDAAO is concerned, ESI/MS analyses identified several complementary peptides with the different proteases (Table 1). Only for Glu-C digestion, the complementary peptide was not detected and, analogously to that described above for pLG72 digestion with Glu-C and subtilisin, we can consider E336 as a primary site of proteolysis, as the complementary peptide is relatively small (11 residues). Figure 1 shows the position of the corresponding cleavage sites (located at F167 and N180) as well as the sites recognized by trypsin (R297), chymotrypsin (Y35, Y55, and L296), and Glu-C (E336). Interestingly, all of them differ from those observed with the same proteases on hDAAO in the absence of pLG72.

Based on these results, several conclusions can be drawn: (a) hDAAO appears more accessible to proteases in the pLG72-complexed form than as a single protein (a lower enzyme-to-substrate ratio provides optimal digestion of hDAAO in complex with pLG72); and (b) a main conformational change is induced in the hDAAO molecule by forming the complex with pLG72, as deduced by the different patterns of preferential proteolytic sites observed for hDAAO in the presence and in the absence of pLG72. Specifically, the peptide bonds following L189, R191, L194 E249, and L250 that were proteolytically hydrolyzed in the isolated hDAAO were not recognized in the presence of pLG72: in contrast, the Y34, Y55, F167, N180, L296, R297, and E336 sites were recognized in the hDAAO–pLG72 complex only (Fig. 1).

Chemical cross-linking

Cross-links formed between residues of a protein or proteins within a complex can be used as 'molecular rulers' to determine short-distance molecular modeling constraints which allow to elucidate the structures of individual proteins, protein conformational changes, or to provide insights into protein–protein interfaces. We used the homobifunctional cross-linker bis(sulfosuccinimidyl)suberate (BS^3), a cross-linker that preferentially targets not only primary amino groups of lysine side chains and the protein N termini but also hydroxyl groups of serine and threonine side chains [28,29], in the study of the hDAAO–pLG72 complex, following the general strategy outlined in Fig. 2. hDAAO (12.5 μM) and pLG72 (62.5 μM) were mixed

Table 1. Peptides generated by digestion of hDAAO, pLG72, and hDAAO–pLG72 complex with different proteases and identified by ESI-MS analysis after fractionation by RP-HPLC.

Protease (protease/ substrate ratio, w/w)	Identified peptide	Experimental mass value (Da)[a]	Theoretical mass value (Da)	Proteolytic site
hDAAO				
Glu-C (1/500)	1–249	28280.49 ± 1.69	28280.49	E^{249}
	250–347	11211.94 ± 1.03	11211.90	
Subtilisin (1/500)	1–189	21478.68 ± 1.22	21478.33	L^{189}
	190–347	18041.14 ± 0.59	18013.66	
Trypsin (1/100)	1–341	38811.56 ± 1.70	38811.16	R^{341}
	1–191	21763.63 ± 1.46	21762.60	R^{191}
	192–341	17066.90 ± 1.00	17066.50	
Chymotrypsin (1/100)	1–250	28392.60 ± 1.75	28393.20	L^{250}
	251–347	11098.27 ± 0.37	11098.70	
	1–194	22089.81 ± 1.99	22088.01	L^{194}
	195–347	17404.48 ± 1.75	17403.97	
	1–189	21476.70 ± 1.53	21478.33	L^{189}
	190–347	18013.41 ± 1.60	18013.66	
pLG72				
Glu-C (1/5000)	1–146	17347.57 ± 1.22	17948.66	E^{146}
Subtilisin (1/2000)	1–150	17751.44 ± 1.51	17751.11	T^{150}
	1–116	13643.55 ± 0.99	13642.59	Y^{116}
	117–153	4454.52 ± 1.00	4454.89	
Trypsin (1/2000)	1–128	15110.15 ± 1.49	15109.22	R^{128}
	129–153	2988.58 ± 0.15	2988.28	
Chymotrypsin (1/2000)	1–61	7030.38 ± 0.38	7030.08	W^{61}
	62–153	11066.37 ± 0.73	11067.41	
	1–130	15908.85 ± 1.12	15908.20	W^{130}
	135–153	2188.96 ± 1.40	2189.34	
hDAAO-pLG72 complex				
Glu-C (1/2000)	1–336	38198.09 ± 1.10	38198.39	E^{336}
Subtilisin (1/10 000)	1–167	19237.07 ± 0.82	19236.82	F^{167}
	168–347	20255.54.±1.81	20255.16	
	1–180	20619.58 ± 0.84	20619.31	N^{180}
	181–347	18872.35 ± 0.64	18872.69	
Trypsin (1/2000)	1–297	34004.15 ± 1.51	34003.70	R^{297}
	298–347	5488.24 ± 0.32	5488.28	
Chymotrypsin (1/2000)	1–35	3851.66 ± 0.13	3851.62	Y^{35}
	36–347	35640.87 ± 1.0	35640.35	
	1–55	6056.99 ± 0.5	6057.07	Y^{55}
	56–347	33434.86 ± 1.48	33434.90	
	1–296	33846.89 ± 1.39	33847.51	L^{296}
	297–347	5644.50 ± 0.43	5644.47	

[a] Experimental mass value ± standard deviation.

(at 1 : 5 subunit molar ratio) and incubated for 15 min and then cross-linked by adding 50-fold molar excess of BS^3 (with respect to hDAAO monomers and under optimized conditions). Electrophoretic and immunodetection analysis of the reaction mixture revealed the presence of a band at ~ 75 kDa positive to both anti-hDAAO and anti-pLG72 antibodies (Fig. 2), thus suggesting a covalent hDAAO–pLG72 complex formation following BS^3 treatment.

In order to identify the cross-linking sites, a gel-free strategy was adopted: the reaction mixture was desalted, carboxyamidomethylated, trypsin digested, and analyzed by LC-MSMS. In order to search for species of low abundance, such as those expected from cross-linked peptides, an exclusion list of signals arising from linear trypsin-digested peptides from the single proteins was set up and inserted in the LC-MSMS program, and the open mass modification strategy developed by [30], based on Batch-Tag, MS-Bridge, and MS-Product tools within the PROTEIN PROSPECTOR package (http://prospector.ucsf.edu/prospector, University of California, San Francisco, CA, USA), was used. Table 2 reports the peptides modified upon treatment with BS^3 in the hDAAO–pLG72 complex. All putative cross-linkings were verified by manual inspection of the corresponding MS/MS spectrum. One

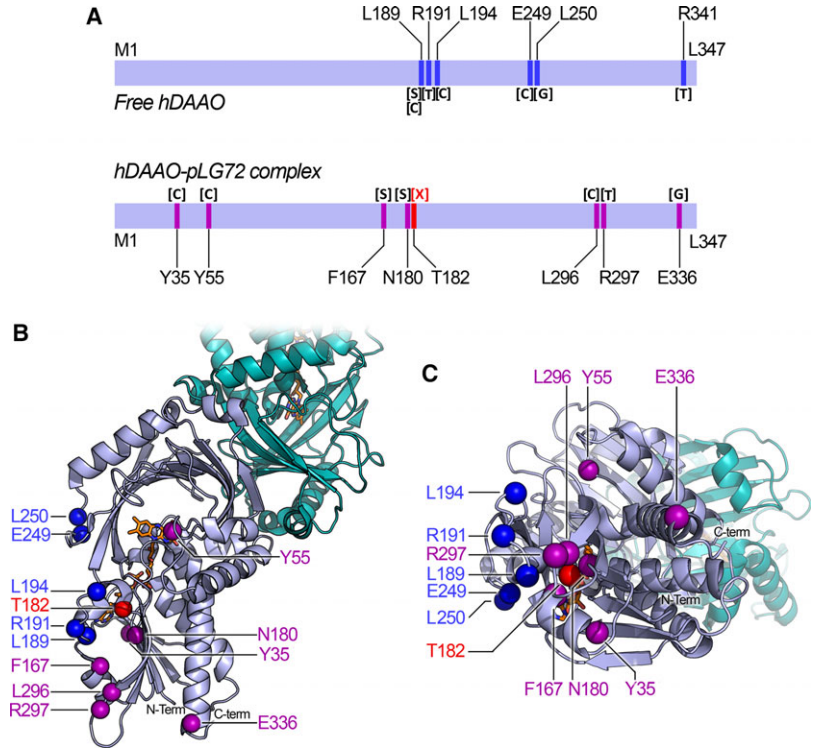

Fig. 1. Proteolysis of hDAAO. (A) Schematic representation of preferential proteolytic sites in hDAAO alone and in the presence of pLG72 (indicated by blue and purple bars, respectively). C = chymotrypsin; S = subtilisin; T = trypsin; G = endoprotease Glu-C; X = SB^3 cross-link (red bar). (B, C) Representation of the sites of proteolysis (spheres) within the three-dimensional structure of hDAAO homodimer (pdb code 2du8); colors as in panel A.

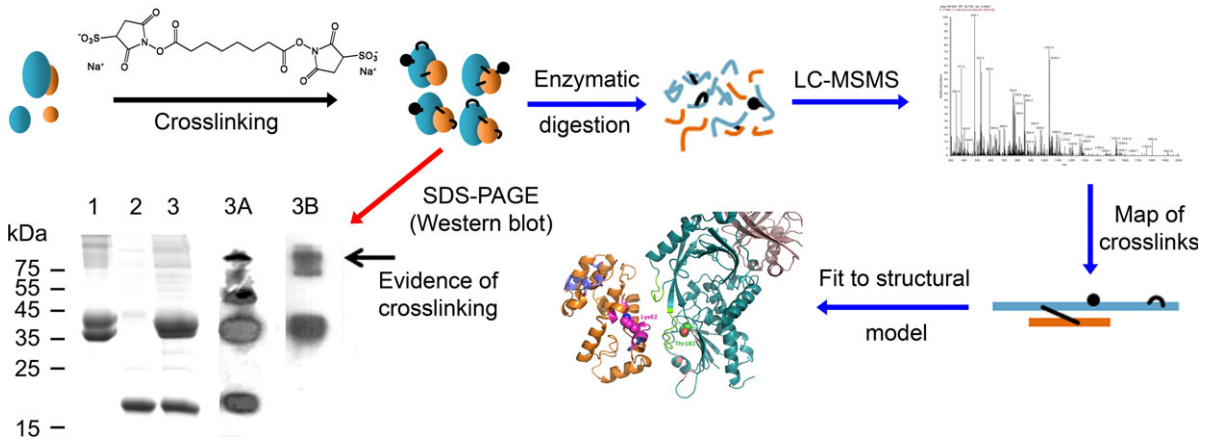

Fig. 2. Scheme of the strategy employed for the identification of the regions involved in hDAAO–pLG72 complex formation by means of cross-linking based on BS^3. Red arrow: gel-based approach showing the electrophoretic analysis of 12.5 μM hDAAO (lane 1), 62.5 μM pLG72 (lane 2), and the corresponding hDAAO–pLG72 complex (at 1 : 5 subunit molar ratio, lane 3) incubated for 15 min and then cross-linked by adding 625 μM BS^3. Lane 3 was also analyzed by western blot using anti-hDAAO (3A) and anti-pLG72 antibodies (3B): besides some protein bands related to intramolecular cross-links occurring within both hDAAO and pLG72, immunodetection analyses revealed that the band at ~ 75 kDa (arrow) was positive to both antibodies. Blue arrows: in solution, gel-free procedure.

cross-link between hDAAO and pLG72 was identified, as inferred by the triple-charged ions at 943.45 (corresponding to the experimental MH^+ value 2828.35) interpreted as the hDAAO peptide 173–191 linked to the pLG72 fragment 59–63 (theoretical MH^+ value 2828.42 Da), besides several dead-end modifications

(namely, the abortive modification of peptides occurring when only one arm of the bifunctional cross-linking agent reacts) and some internal cross-linkings both in pLG72 and hDAAO. Figure 3 shows the fragmentation spectrum where several ions of the y-ion and b-ion series confirmed the identity of the $hDAAO^{173–191}$ peptide. Fragmentation spectra of cross-linked peptides often suffer from the fact that collisional activation energy typically favors the formation of product ions from only one of the two constituent peptides [31], generally the longer one. The double-charged ions y_{12}^{2+}, y_{13}^{2+}, y_{14}^{2+}, y_{15}^{2+}, y_{16}^{2+}, accounting for fragments of the 173–191 hDAAO peptide cross-linked with peptide 53–63 from pLG72, were considered to be the key signals to confirm the linkage between the two proteins through K62 pLG72 and T182 hDAAO. It is worth noting that these cross-linked fragments are doubly charged, as the presence of two connected peptide moieties might suggest.

Model of pLG72 tertiary structure

As the experimental three-dimensional structure of pLG72 has not been solved, a model of its tertiary structure was built by homology modeling using the I-TASSER server. Five potential models based on a three-dimensional structure of templates belonging to small α-helix proteins (e.g., T4 lysozyme) were produced. The reliability of the I-TASSER models was evaluated based on: (a) the position of the exposed regions identified by limited proteolysis (in the pLG72-VA model all cleavage sites are located in the protein surface); (b) the position of the residue identified by cross-linking with hDAAO (notably, in the pLG72-VA model, the residues K4, K36, K46, K62, and L120 labeled by BS^3 are all located on the protein surface and the side chains of M1 and K4 are juxtaposed to yield the internal cross-link); (c) the computational analysis of the quality of the models by the SAVES metaserver. Indeed, the selected model (pLG72-VA, Fig. 4A) shows an α-helix content of ~ 62%, which is in good agreement with the experimental value obtained by CD analysis (~ 73%) [20]. pLG72-VA significantly differs from the model proposed by [32,33]: the latter was built using 1zca as template, a protein that shares a negligible sequence identity with pLG72 (an overall identity of 10.3% with a maximal identity of 27%, considering only ~ 30% of the template, and a blast E-value of 4.9). Notably, *in silico* molecular docking analysis showed that the pLG72-VA model binds chlorpromazine (CPZ) (Fig. 4B), an aliphatic phenothiazine drug known for its ability to interact with pLG72, forming a complex possessing a predicted $K_d \sim 11$ μM (predicted binding energy: 6.6 kcal·mol^{-1}) close to the experimental value (~ 5 μM) [12,13]. CPZ is bound to pLG72-VA by hydrophobic interactions only and with the Cl atom solvent exposed; see Fig. 4B.

Furthermore, the availability of the pLG72 structure model and of the experimental structure of hDAAO made it possible to predict their mode of interaction by protein–protein molecular docking using the server ZDOCK. As the residues K62 (pLG72) and T182 (hDAAO) were identified by cross-linking experiments, only the complexes in which these two residues were close to the contact surfaces were considered by ZDOCK. Three alternative hDAAO–pLG72 complexes were produced. The one showing the highest agreement with limited proteolysis analysis protection data (see Fig. 1 and Table 1) and possessing the highest surface of contact between the two proteins was considered for further analysis (Fig. 4C,D). In the proposed mode of interaction, the distance between the -NH_2 group of K62 of pLG72 and the OH-group of T182 of hDAAO is 12.2 Å with a distance between the C-atom of the corresponding residues of 17 Å. These values are within the experimentally observed distance constraint for the BS^3 reagent (which has a linker arm 11.4 Å long) that is 26–30 Å between C-atom of the linked residues [34].

From the calculation of the solvent-accessible surface, the predicted hDAAO–pLG72 complex excludes 1038 Å^2 in hDAAO and 1072 Å^2 in pLG72 from solvent contact, pointing to a stable interaction.

Design of C-terminal truncated forms of pLG72

Four truncated variants of pLG72 were designed by *in silico* analyses. Analysis of full-length pLG72 by employing PSIPRED software revealed a highly unstructured C-terminal region (Fig. 5A): in agreement with MobiDB analysis (data not shown), the $pLG72^{1–123}$ variant was selected in order to obtain a more stable recombinant protein lacking the disordered C-terminal tail. With the same purpose, an even shorter protein form was designed: $pLG72^{1–94}$. The latter variant lacks the last 59 residues which are conserved in the products of isoforms 1–3 of G72 gene transcript (GI:126362975, GI:240120173, GI:240120029, respectively) [35], and eventually correspond to the form of the human protein expressed in G72 transgenic mice, reported as AFB69504.1 in the NCBI database (GI:377551785) [36]. The protein corresponding to $pLG72^{72–153}$ is recognized as an interaction domain with DAAO by the Pfam database (PF15199, http://

Table 2. BS^3-modified peptides. The measured precursor masses are included, along with the error of the measured precursor ion compared to the theoretical mass. Peptide sequences are reported with the position within the protein and the flanking residues. Modified residues are reported in bold, dead-end modified residues are underlined, cross-linked residues are connected by lines.

m/z	Charge	Experimental MH^+	Matched MH^+	Error (p.p.m.)[a]	Peptide sequence
943.45	+3	2828.35	2828.41	21	(R)^{173}EGADVIVNC(Cam)**T**GVWAGALQR^{191}(D) hDAAO | (K)^{59}EGW**K**R^{63}(R) pLG72
627.37	+2	1253.74	1253.75	8	(R)^{333}ILEE**KK**LSR^{341}(M) hDAAO
418.58	+3	1253.74			
666.35	+2	1331.68	1331.68	–	(R)^{163}**K**VES**S**FEEVAR^{172}(E) hDAAO
572.33	+3	1714.97	1714.98	6	(-)^{1}**M**R^{2}(V) hDAAO | (R)^{333}ILEE**K**<u>**K**</u>LSR^{341}(M) hDAAO
577.66	+3	1730.97	1730.97	–	(-)^{1}**M(ox)**R^{2}(V) hDAAO | (R)^{333}ILEE**K**<u>**K**</u>LSR^{341}(M) hDAAO
442.24	+3	1324.71	1324.72	7.5	(-)^{1}**M**R^{2}(V) hDAAO | (R)^{156}GV**K**FFQR^{162}(K) hDAAO
546.28	+3	1636.83	1636.84	6	(-)^{1}**M**R^{2}(V) hDAAO | (R)^{163}**K**VESFEEVAR^{172}(E) hDAAO
551.61	+3	1652.83	1652.83	–	(-)^{1}**M**(ox)R^{2}(V) hDAAO | (R)^{163}**K**VESFEEVAR^{172}(E) hDAAO
495.61	+3	1484.82	1484.82	–	(-)^{1}**M**R^{2}(V) hDAAO | (R)^{266}LEPTL**K**NAR^{274}(I) hDAAO
590.79	+4	2360.14		59	(-)^{1}**M**R^{2}(V) hDAAO | (R)^{23}YHSVLQPLDI**K**VYADR^{38}(F) hDAAO
616.32	+3	1846.94	1846.94	–	(-)^{1}**M**R^{2}(V) hDAAO | (R)^{200}GQIM**K**VDAPWMK^{211}(H) hDAAO
734.89	+4	2936.55	2936.57	7	(R)^{23}YHSVLQPLDI**K**VYADR^{38}(F) hDAAO | (R)^{156}GV**K**FFQR^{162}(K) hDAAO
459.28	+4	1834.09	1834.01	44	(R)^{163}**K**VESFEEVAR^{172}(E) hDAAO | (K)^{338}**K**LSR^{341}(M) hDAAO
791.44	+3	2372.31	2372.28	13	(R)^{163}**K**VESFEEVAR^{172}(E) hDAAO | (R)^{266}LEPTL**K**NAR^{274}(I) hDAAO
539.55	+4	2155.17	2155.18	5	(R)^{200}GQIM**K**VDAPWMK^{211}(H) hDAAO | (R)^{116}**K**LTPR^{120}(E) hDAAO
945.49	+2	1889.98	1889.99	5	(-)^{1}**M**LE**K**LMGADSLQLFR^{15}(S) pLG72
953.49	+2	1905.97	1905.98	5	(-)^{1}**M**LE**K**LM(ox)GADSLQLFR^{15}(S) pLG72
715.86	+4	2860.41	2860.45	14	(K)^{37}SENSLNSIA**K**ETEEGR^{52}(E) pLG72 | (K)^{59}EGW**K**R^{63}(R) pLG72
691.70	+3	2073.10	2073.10	–	(R)^{23}YHSVLQPLDI<u>**K**</u>VYADR^{38}(F) hDAAO
1037.05	+2	2073.10			
490.27	+3	1468.79	1468.80	7	(R)^{23}YH<u>**S**</u>VLQPLDIK^{33}(V) hDAAO
385.74	+2	770.48	770.48	–	(R)^{116}<u>**K**</u>LTPR^{120}(E) hDAAO
519.29	+2	1037.58	1037.58	–	(R)^{156}GV<u>**K**</u>FFQR^{162}(K) hDAAO

Table 2. (Continued)

m/z	Charge	Experimental MH^+	Matched MH^+	Error (p.p.m.)[a]	Peptide sequence
675.35	+2	1349.69	1349.69	–	(R)^{163}**K**VESFEEVAR^{172}(E) hDAAO
780.40	+2	1559.80	1559.80	–	(R)^{200}GQIM**K**VDAPWMK^{211}(H) hDAAO
787.91	+2	1574.81	1574.81	–	(R)^{200}GQIM(ox)**K**VDAPWMK^{211}(H) hDAAO
599.34	+2	1197.68	1197.68	–	(R)^{266}LEPTL**K**NAR^{274}(I) hDAAO
399.90	+3	1197.68		–	
424.59	+3	1271.74	1271.76	16	(R)^{333}ILEE**KK**LSR^{341}(M) hDAAO
714.41	+2	1427.82	1427.83	7	(R)^{333}ILEE**KK**LSR^{341}(M) hDAAO
419.21	+2	837.41	837.42	12	(R)^{342}MPP**S**HL^{347}(-) hDAAO
812.76	+3	2436.27	2436.28	4	(R)^{192}DPLLQPGRGQIM**K**VDAPWMK^{211}(H) hDAAO
954.50	+2	1908.00	1908.00	–	(-)^{1}MLE**K**LMGADSLQLFR^{15}(S) pLG72
1032.54	+2	2064.07	2064.07	–	(-)^{1}**M**LE**K**LMGADSLQLFR^{15}(S) pLG72
930.52	+2	1860.03	1860.03	–	(R)^{31}SILLS**K**SENSLNSIAK^{46}(E) pLG72
960.46	+2	1919.92	1919.92	–	(K)^{37}SENSLNSIA**K**ETEEGR^{52}(E) pLG72
881.42	+2	1761.83	1761.83	–	(R)^{110}NYEFLAYEAS**K**DR^{122}(R) pLG72

[a] The reported error is calculated as the difference between the experimental and the theoretical mass values in p.p.m.

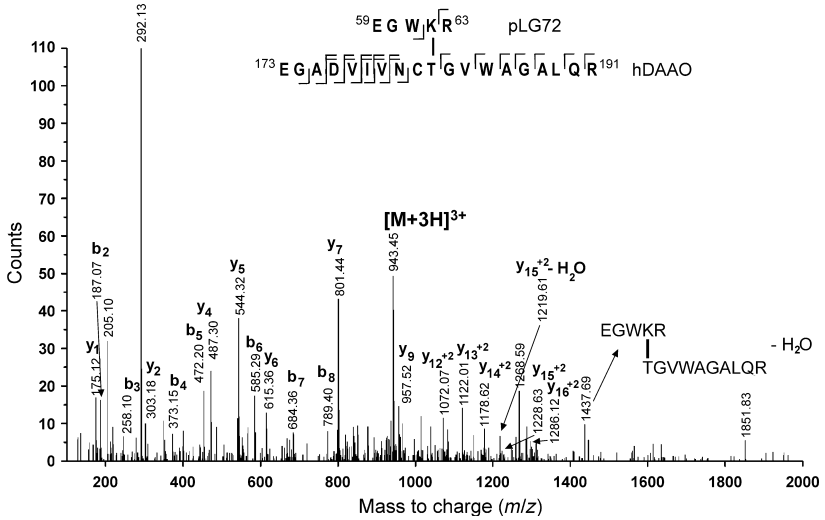

Fig. 3. MS/MS spectra of the triply charged ions at *m/z* 943.45 (experimental $[MH]^+$ *m/z* 2828.35, calculated $[MH]^+$ *m/z* 2828.41) interpreted as peptide 173–191 of hDAAO linked to peptide 59–63 of pLG72 (see inset). The product ions are indicated with the observed mass.

pfam.xfam.org/): this observation suggests that it could correspond to a structurally and functionally stable domain. Finally, pLG72$^{1–64}$ has been designed in response to results gathered from the experiments of this work with the aim to identify the minimal interacting N-terminal region excluding the overlapping sequence between the variant pLG72$^{1–94}$ and pLG72$^{72–153}$, see Fig. 5B.

In order to investigate the role played by the C-terminal tail, a synthetic peptide encompassing the region from 122 to 153 was used to evaluate the binding and the inhibitory effect on hDAAO.

Properties of pLG72 deletion forms

The deletion variants of pLG72 were expressed in *E. coli* using the pETM11 plasmid and the same conditions previously used for the full-length protein [20]. Recombinant pLG72 variants largely accumulated as inclusion bodies and were solubilized and refolded in the presence of the anionic detergent NLS, reaching a > 95% degree of purity and a yield of 155–525 mg pure protein per liter fermentation broth.

The pLG72 variants showed absorbance spectra differing in wavelength of maximum intensity and in

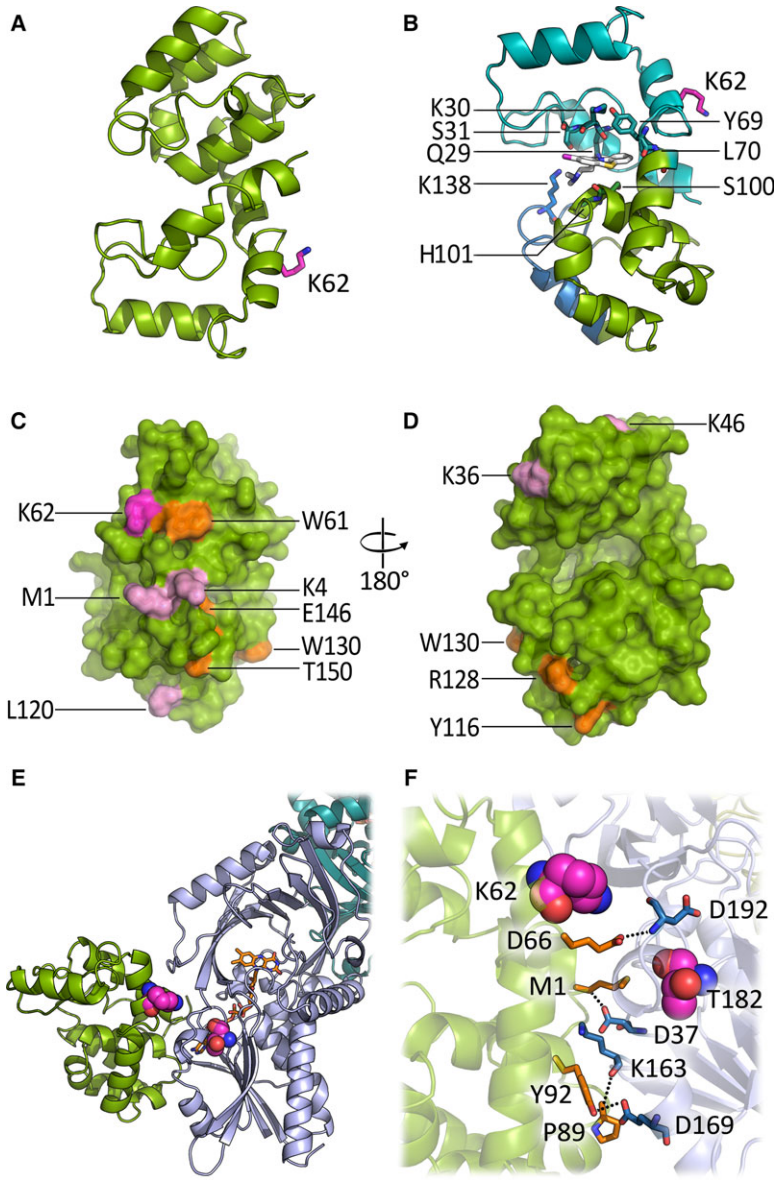

Fig. 4. Homology model of pLG72 and proposed mode of interaction with CPZ and hDAAO. (A) Model of pLG72-VA, produced by I-TASSER server using the structure of T4 lysozyme (pdb code 217l) as template; residue K62, identified by cross-linking experiments with hDAAO, is represented in purple. (B) Mode of CPZ binding to pLG72-VA obtained by automated molecular docking simulations using AUTODOCK VINA [50]; the ligand is shown in van der Waals and sticks representation (white atoms), orientation of pLG72-VA is reversed in comparison with panel A. The dark blue depicts the region deleted in $pLG72^{1–123}$, and light blue depicts the region deleted in $pLG72^{72–153}$. Residues forming noncovalent interactions with CPZ are shown as sticks. (C) Surface representation of pLG72-VA model: proteolytic sites are shown in orange, dead-end modified residues by BS^3 are shown in pink and cross-linked K62 residue is shown in purple. M1 and K4 form an intramolecular cross-link (see Tables 1 and 2 for details). (D) Model of hDAAO–pLG72 complex as predicted by ZDOCK server; pLG72-VA is in green, hDAAO monomers in violet and cyan. (E) Details of the H-bonds formed at the contact interface. Residues identified by cross-linking experiments are shown in van der Waals radius representation, and residues forming H-bonds at the interface are shown as sticks; dotted lines represent hydrogen bonds.

extinction coefficient (Table 3). Indeed, different protein fluorescence spectra were recorded for the deletion variants, depending on the number of Trp residues (three for the full-length pLG72, two for the 1–123, 1–94, and 72–153 variants, and one for the 1–64 variant) and the microenvironment surrounding the aromatic amino acid probe—in particular, compare the different fluorescence yields of the three pLG72 proteins

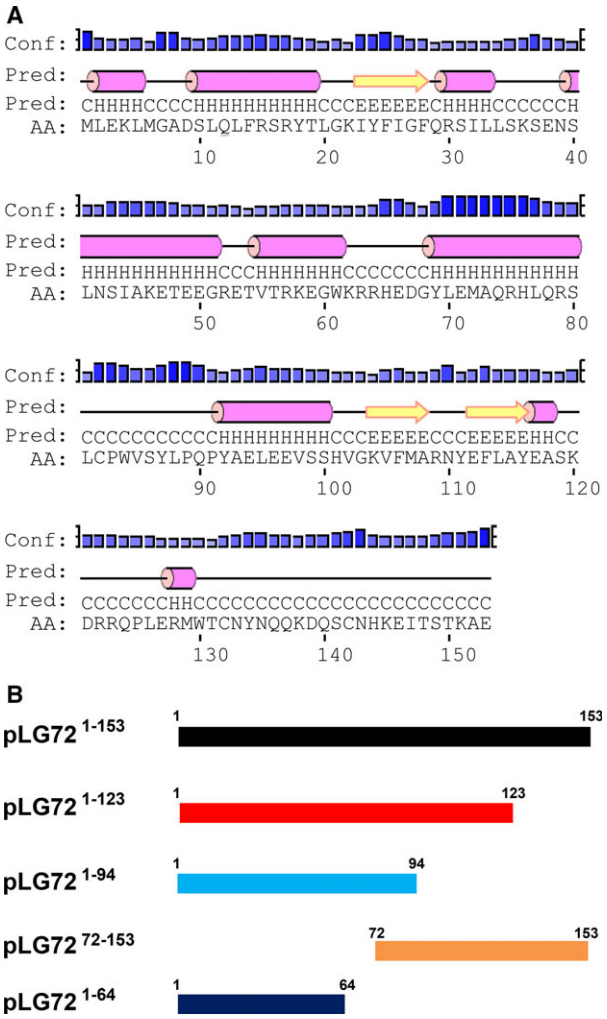

Fig. 5. Deletion variants of pLG72. (A) Psipred analysis of disordered regions in pLG72. Conf = confidence of prediction; C = coil; E = strand; H = helix. (B) Schematic representation of the pLG72 variants produced in this work.

containing two Trp residues (Fig. 6A). The fluorescence spectrum of polypeptide 122–153 showed a blue shift (maximum at ~ 360 nm) and an intensity similar to that of the longer pLG72$^{72–153}$ variant, although it contains a single Trp residue: this indicates that W130 is a solvent exposed in the polypeptide corresponding to the pLG72 C-terminal tail. Similarly, the near-UV CD spectra of pLG72 deletion variants resembled the one recorded for the full-length protein, differing in intensity of the positive peaks at ~ 265 nm (Fig. 6B). A similar content of secondary structure elements (mainly α-helices) for all the pLG72 forms investigated was apparent by the far-UV CD spectra, with the main exception of the 122–153 polypeptide (Fig. 6C).

The thermal stability of the tertiary structure of pLG72 was investigated following the CD signal at 265 nm. As compared to the full-length protein, the lowest stability was apparent for the pLG72$^{1–94}$ variant and the highest T_m was observed for the shorter variant 1–64 (showing a 15 °C increase in melting temperature; Table 3).

When the oligomeric state was analyzed by size-exclusion chromatography, the full-length pLG72 showed a main peak corresponding to a dimeric form of the protein (K_{AV} ~ 0.442, M_r = 43.8 kDa) and a minor peak at high molecular mass (K_{AV} ~ 0.009, M_r ~ 740 kDa): their relative intensity was approximately 2.5 : 1.0 [12]. A similar elution profile was observed for all deletion variants, the only exception being the pLG72$^{1–94}$: in the latter case, the peak at high molecular mass was absent and a new peak corresponding to a hexameric state (K_{AV} ~ 0.29, M_r = 117 kDa) was apparent (not shown). For all pLG72 variants, DLS analysis of the main peak eluted from size-exclusion chromatography indicated the proteins were in a dimeric state.

pLG72 was reported to bind large, aromatic compounds such as CPZ, a well-known drug used to treat schizophrenia [14]. All deletion variants interacted with CPZ with an affinity similar to the full-length pLG72 (Table 3), in agreement with the structural model showing that it binds to a hydrophobic pocket without forming specific noncovalent interactions (Fig. 4B). The lowest affinity was observed for pLG72$^{72–153}$, which lacks a region involved in CPZ binding in our model.

hDAAO binding to pLG72 variants

The interaction of full-length pLG72 to hDAAO generates a ~ 200 kDa complex formed by two hDAAO homodimers and two pLG72 monomers (K_{AV} ~ 0.195) [12,13]. Size-exclusion chromatography of a mixture of hDAAO and pLG72 proteins confirmed production of the ~ 200-kDa complex for all deletion variants (not shown). The interaction was then investigated by SPR technology: hDAAO was immobilized on the chip surface and all pLG72 variants were used as free analytes. A low micromolar dissociation constant value for the hDAAO–pLG72 variants complex was determined (Table 3 and Fig. 7). These results show that deletion of the C-terminal tail positively affects the interaction with hDAAO; conversely, the lack of the N-terminal region slightly negatively influences the hDAAO–pLG72 interaction (resulting in a 1.4-fold weaker binding; Table 3). Interestingly, the 122–153 polypeptide did bind aspecifically to hDAAO (K_d >> 10 μM, Fig. 7).

Table 3. Comparison of properties of full-length and deletion variants of pLG72.

pLG72 forms (molecular mass, Da)	Wavelength of maximal absorbance, nm (ε, $mM^{-1}\cdot cm^{-1}$)	$K_{d,CPZ}$ (μM)[a]	$K_{d,hDAAO}$ (μM)[a]	T_m (°C)[a]	Molecular mass by LS (Da)[a]
1–153 (18 079)	268 (34.780)	1.56 ± 0.21	2.6 ± 0.4	59.2 ± 2.7	35 075 ± 315
1–123 (17 576)	268 (26.125)	0.82 ± 0.27	0.40 ± 0.05	66.3 ± 11.0	33 818 ± 461
1–94 (14 162)	265 (23.490)	0.95 ± 0.29	2.1 ± 0.3	50.9 ± 4.6	28 307 ± 56
72–153 (12 743)	263 (24.280)	2.33 ± 0.33	3.7 ± 0.1	64.6 ± 1.2	24 815 ± 175
1–64 (10 526)	259 (13.715)	1.02 ± 0.28	2.2 ± 0.2	73.7 ± 1.4	20 707 ± 82

[a] Mean ± standard deviation, $n = 3$.

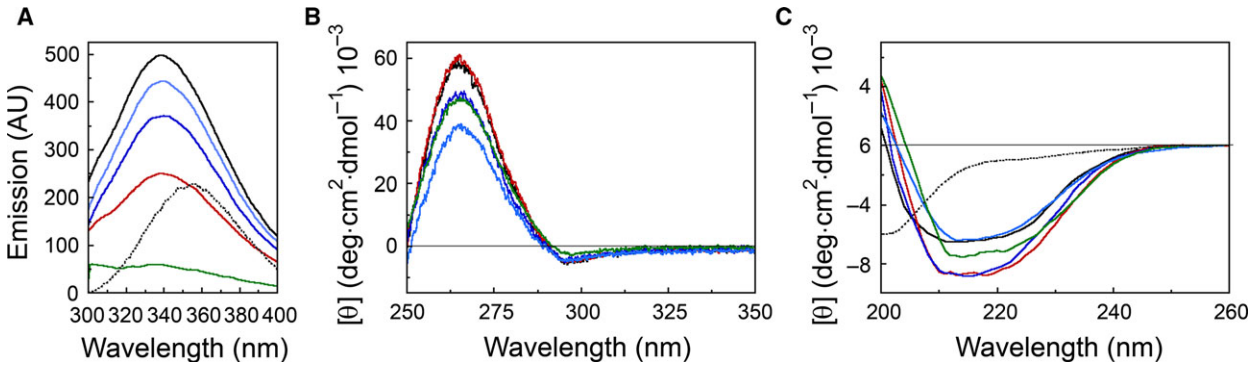

Fig. 6. Spectral properties of pLG72 variants. (A) Fluorescence spectra; (B) near-UV CD spectra; (C) far-UV CD spectra. Full-length pLG72 (black); $pLG72^{1–123}$ (blue); $pLG72^{1–94}$ (light blue); $pLG72^{72–153}$ (red); $pLG72^{1–64}$ (green); $pLG72^{122–153}$ (dotted black).

We previously demonstrated that the main effect of pLG72 binding to hDAAO was a slow inactivation of the flavoenzyme [12]. We now investigated the effect of 0.5-, 1-, 2-, and 4-fold molar excess of the different pLG72 deletion variants on hDAAO activity after 30 min of incubation. At a 1 : 2 hDAAO:pLG72 ratio, all the deletion variants inhibited the flavoenzyme to a limited extent: 25–50% of inhibition versus > 80% observed using the full-length pLG72 (Fig. 8). At a four-fold pLG72 molar excess, the 1–64 and 1–94 shorter variants were significantly less effective in inhibiting hDAAO than the $pLG72^{72–153}$ (the one showing the lowest affinity for hDAAO), the $pLG72^{1–123}$, and the full-length protein. On the other hand, the short polypeptide 122–153 did not affect hDAAO activity at any molar ratio, supporting aspecific binding.

Discussion

Schizophrenia is a complex neurodevelopmental disorder [37] in which susceptibility genes are assumed to play a specific role in the pathophysiology of the disease via abnormal synaptic connectivity [38]. Among the proposed susceptibility genes [39–41], we have focused in past years on the one involved in the catabolism of the neuromodulator D-serine, a full agonist at the glycine site of the NMDAR [42], namely, DAAO and its interacting partner pLG72 [3]. The human flavoenzyme DAAO was the object of a plethora of investigations [12–15,20,27], while little is known about the product of the primate-specific *G72* gene [17,43]. pLG72 is a small protein (153 amino acids) assumed to localize on the cytosolic side of the outer mitochondrial membrane where it can interact with neosynthesized hDAAO before it targets peroxisomes [14]. pLG72 was proposed as a 'negative chaperone' [44], i.e., a modulator of the protein conformation that negatively affects enzyme activity, as it promotes enzyme inactivation and degradation [12–15].

In the absence of atomic resolution data, orthogonal structural information is needed to accurately interpret the findings; therefore, we employed low-resolution

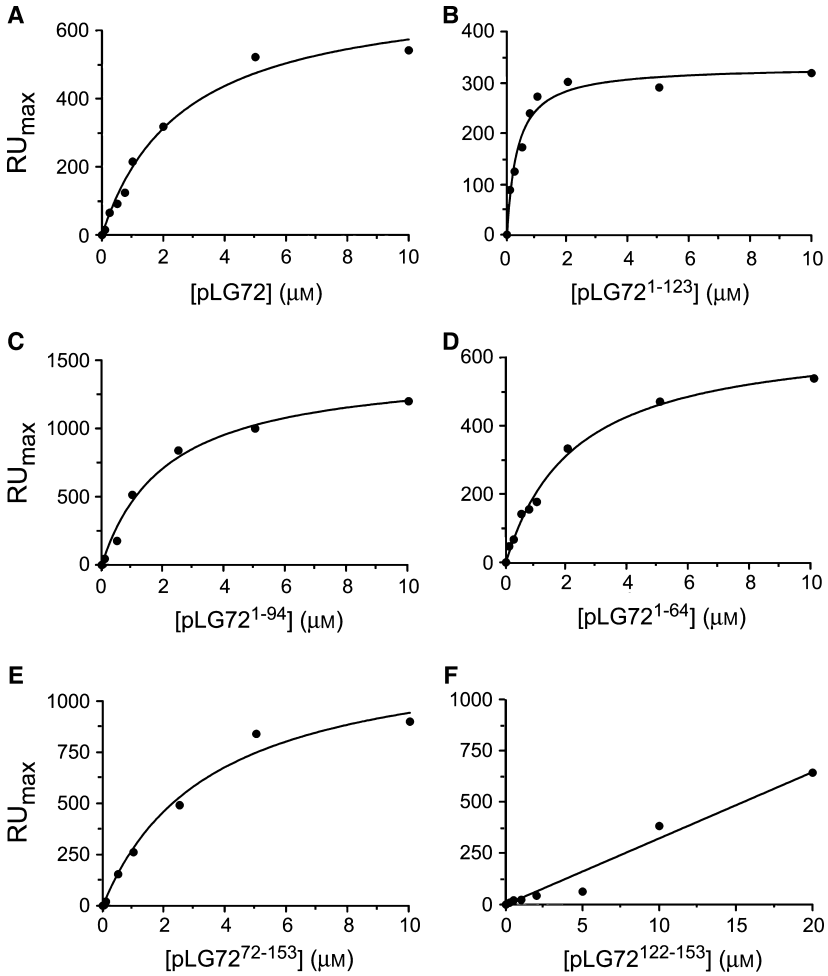

Fig. 7. SPR experiments of the interaction of hDAAO (immobilized on the chip) with full-length pLG72 (A) and the variants pLG72$^{1–123}$ (B), pLG72$^{1–94}$ (C), pLG72$^{1–64}$ (D), pLG72$^{72–153}$ (E), and pLG72$^{122–153}$ (F).

techniques, such as those based on the coupling of classical biochemical approaches (limited proteolysis and chemical cross-linking) with mass spectrometric techniques, to provide an overall characterization of the surface topology of the hDAAO–pLG72 complex. Controlled experimental conditions of limited proteolysis produce specific cleavages on the exposed/flexible regions of the protein which are identified by the mass of the resulting complementary peptides. The evidence that, in complex with pLG72, hDAAO shows a higher sensitivity to proteolysis suggests that this interaction decreases the overall compactness of the flavoenzyme, supporting previous results [13]. This is a peculiar observation as the opposite is often observed, i.e., a decrease in the overall flexibility and accessibility of individual proteins when they combine to form a complex. Conformational changes occurred both within the C-terminal tail, which became less flexible and exposed, as well as at the N-terminal end of the flavoenzyme, which was only cleavable in the presence of pLG72 (Fig. 1). Cross-linking experiments identified the single covalent interaction between T182 in hDAAO and K62 in pLG72. Notably, K62 is in close proximity to the site recognized by chymotrypsin in free pLG72 and thus likely exposed on the protein surface. The information gathered from both structural approaches were used to select the mode of interaction between the known three-dimensional structure of hDAAO and the pLG72 model (predicted to be an α protein; see Fig. 4).

The reliability of the pLG72 tertiary structure model is supported by its *in silico* ability to bind CPZ in docking analyses and the experimental evidence of decreased affinity for this aromatic ligand in the pLG72$^{72–153}$ variant lacking part of the residues contributing to the binding site (Table 3 and Fig. 4B). In order to validate this model, four

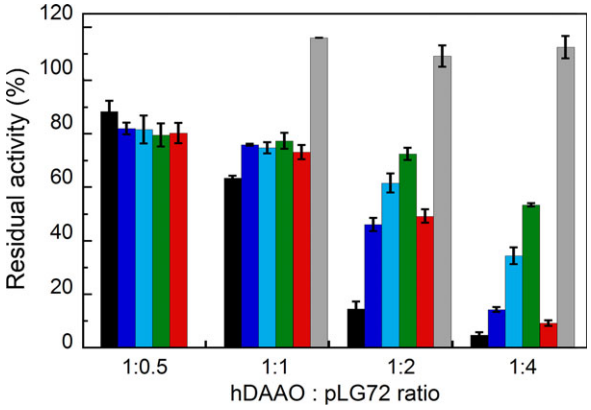

Fig. 8. Effect of increasing amounts of pLG72 on the activity of hDAAO. The residual activity was assayed 30 min after incubation of 13 μM hDAAO and pLG72 (at the indicated molar ratios), at 25 °C. The activity of hDAAO alone is referred as 100%. Full-length pLG72 (black); $pLG72^{1–123}$ (blue); $pLG72^{1–94}$ (light blue); $pLG72^{1–64}$ (green); $pLG72^{72–153}$ (red); $pLG72^{122–153}$ (gray). n.d. = not determined. Bars represent mean ± SD, $n = 4$.

deletion variants were produced. The three pLG72 variants lacking incremental regions at the C terminus, as well as the form lacking the 71 N-terminal residues, are dimeric in solution, contain secondary and tertiary structures (Fig. 6), and interact with hDAAO. As shown in Fig. 4E, specific residues of pLG72 belonging to protein loops in the 1–92 region seem to be explicitly involved in the interaction with hDAAO: as a result, the strongest decrease in affinity for hDAAO was apparent for the $pLG72^{72–153}$ N-terminally deleted form lacking K62 (i.e., of the residue identified by cross-linking experiments). According to the proposed protein interaction mode reported in Fig. 4D, only the last three C-terminal residues of pLG72 interact with hDAAO, thus explaining the slight change in binding affinity observed for the pLG72 C-terminal deletion variants. Indeed, although the deletion of residues 65–153 results into the loss of a significant portion of interface surface, the buried solvent-accessible area in the $pLG72^{1–64}$ variant–hDAAO complex is only halved in comparison to the full-length protein (i.e., 520 versus 1057 $Å^2$, respectively, as calculated by PDBEPISA) [45]. Furthermore, we cannot exclude a different conformation of these shorter variants in comparison with the wild-type pLG72. Deletion of the C-terminal tail of pLG72 in the 1–123 variant, the region with the highest degree of disorder [46,47], results into a more stable protein (T_m is 7 °C higher) which binds to hDAAO with a higher affinity (K_d is 0.4 μM) in comparison to the full-length pLG72.

On the other hand, the hDAAO inhibitory capacity of pLG72 variants is difficult to reconciliate with the proposed pLG72 model and hDAAO interaction mode. Actually, the lowest hDAAO inhibitory capacity is apparent for the shorter N-terminal pLG72 forms (1–64 and 1–94), while the inhibitory efficacy of $pLG72^{72–153}$ was largely preserved (Fig. 8). Altogether, the C-terminal half of pLG72 sequence seems to be required to induce the alterations in hDAAO conformation associated with loss of its catalytic function. Further investigations such as cross-linking and limited proteolysis experiments of the $pLG72^{1–64}$ and $pLG72^{72–153}$ with hDAAO will be required to refine/validate the proposed pLG72 model.

Our results with the $pLG72^{122–153}$ peptide differ from the ones gathered by [35] that reported a stronger interaction with hDAAO as compared to the full-length pLG72: the latter result was based on a nonquantitative pull-down experiment employing a biotinylated pLG72 form while our evidence arises from size-exclusion chromatography and SPR analyses on the unmodified protein. Indeed, the same authors reported an increase in hDAAO activity at increasing pLG72 concentrations. The main difference with our analyses was related to the enzymatic assay that was performed without free flavin adenine dinucleotide (FAD). The cofactor is absolutely required in the assay mixture as FAD dissociation constant is 8 μM for hDAAO [48]: in the absence of exogenous FAD, large part of hDAAO is present in solution in the apoprotein, inactive form and measurement of the initial velocity assays the effect of pLG72 on the apoprotein–holoenzyme equilibrium. As compared to the wild-type counterpart, for the $pLG72^{122–153}$ peptide, a small, ~ 20% increase in hDAAO activity using 10 μM pLG72 was reported by [35], a value resembling the one we also observed (10–15%, Fig. 8): this result highlights that $pLG72^{122–153}$ binding does not affect hDAAO conformation.

From a pharmacological point of view, a decrease in inhibitory hDAAO potency of class C compounds (a novel class of inhibitors which act on the flavoenzyme via an allosteric, covalent mechanism) was apparent in the presence of pLG72, consistent with a model in which the hDAAO–pLG72 interface shields the cysteine residues of the flavoenzyme from this modification [44]. The same study identified compounds that were more potent hDAAO inhibitors (class A compounds) when pLG72 was present. Elucidation at the structural level of the mode of hDAAO–pLG72 interaction is quite exciting as it opens up possibilities for designing novel molecules that target the complex and can be more advantageous therapeutically.

Experimental procedures

Cloning, expression, and purification of pLG72-deleted variants

pLG72 variants were produced in *E. coli* using the pETM11 expression vector (Novagene, Merck-Millipore, Billerica, USA). In order to clone the *G72* gene [20] in the pETM11 plasmid, the *Nco*I restriction site present in the sequence of *G72* was removed by using the QuikChange kit (Agilent Technologies, Santa Clara, CA, USA) and the following oligos: Fw: 5′-CAGCGTAGCTTATGCCCTTGGG TTTCGTATTTGCC-3′; Rv: 5′-GGCAAATACGAAACC-CAAGGGCATAAGCTACGCTG-3′. The resulting *G72* gene, corresponding to full-length pLG72, was used as a template for four different mutagenesis reactions, applying the appropriate oligos designed to obtain 5′- or 3′-deleted pLG72 gene. The mutated DNA fragments were inserted into the pETM11 plasmid using the *Nco*I and *Xho*I restriction sites, yielding pLG72 variants containing an N-terminal 6x His tag. All the deletion variants were expressed and purified by following the procedures reported in [20], with slight modifications. The concentration of the purified full-length and deleted pLG72 variants was determined using the experimentally determined extinction coefficient at ~ 270 nm (see Table 3). For mass spectrometry analysis, the final protein preparations were equilibrated in 20 mM sodium pyrophosphate buffer, pH 8.5, 150 mM NaCl, 5% glycerol, 1 mM dithiothreitol (DTT), containing 0.06% *N*-lauroylsarcosine (NLS).

The synthetic peptide encompassing residues from 122 to 153 was purchased from Inbios S.r.l. (Naples, Italy).

DAAO preparation and activity assay

Recombinant hDAAO was expressed in *E. coli* and purified as reported in [48]. For mass spectrometry analysis, the final enzyme preparation was equilibrated in 20 mM sodium pyrophosphate buffer, pH 8.5, 150 mM NaCl, 5% glycerol, and 1 mM DTT, containing 40 μM FAD: the protein was diluted in plain buffer without FAD before use. The concentration of the purified hDAAO was determined using the extinction coefficient at 455 nm (12.2 $mM^{-1}\cdot cm^{-1}$) [48].

DAAO activity was assayed with an oxygen electrode at pH 8.5, air saturation, and 25 °C, using 28 mM D-alanine as substrate in the presence of 0.2 mM FAD.

Complementary proteolysis experiments

Enzymatic hydrolyses of hDAAO, pLG72, and the hDAAO–pLG72 complex were performed at 37 °C in 20 mM sodium pyrophosphate, pH 8.5, 150 mM NaCl, 5% glycerol, 0.06% NLS, and 1 mM DTT, with either trypsin, chymotrypsin, subtilisin, or Glu-C, and at enzyme-to-substrate ratios ranging from 1 : 100 to 1 : 5000 (w/w). The time course of proteolysis was monitored by sampling the reaction mixture at different time intervals (from 1 to 30 min). The reaction was stopped by adding 20% trifluoroacetic acid (TFA) or a denaturing buffer (300 mM Tris/HCl, pH 8.0, 6 M guanidine, 10 mM EDTA) and the incubation mixtures were separated by reverse-phase (RP) HPLC on a Vydac C4 column (250 × 4.6 mm, 300 Å pore size) with a 10–65% acetonitrile linear gradient in 0.1% TFA over 30 min, at a flow rate of 1 $mL\cdot min^{-1}$. Elution was monitored at 220 nm and individual fractions were collected and analyzed by ESI-MS on a ZQ single quadrupole instrument (Waters-Micromass, Milford, MA, USA). Protein solution was injected into the ion source at a flow rate of 10 $\mu L\cdot min^{-1}$. Data were elaborated using the MASSLYNX program (Waters-Micromass). The multiply charged ions of horse heart myoglobin (Sigma-Aldrich, St. Louis, MO, USA, average molecular mass: 16951.5 Da) was used to calibrate the instrument in a separate injection; all masses are reported as average values: an average error of about 50 p.p.m. was observed for the experimental masses in respect to theoretical values.

Cross-linking experiments

Once the optimal protein-to-cross-linker molar ratio was established in preliminary experiments, hDAAO–pLG72 complex cross-linking experiments were carried out on a preparative scale: 3 nmol of hDAAO and 15 nmol of pLG72 were incubated at 37 °C for 15 min in 200 μL of 20 mM Na-HEPES, pH 8.5, 150 mM NaCl, 0.06% NLS, and 1 mM DTT, and then treated with a 50-fold molar excess of BS^3, which contains an amine-reactive *N*-hydroxysulfosuccinimide ester at each end of an eight-carbon spacer arm, for 30 min at 25 °C; the reaction was stopped by adding Tris to a final concentration of 20 mM. The protein sample was desalted by RP-HPLC on a Vydac C4 column with a 25–65% acetonitrile linear gradient in 0.1% TFA over 2 min, at a flow rate of 1 $mL\cdot min^{-1}$. Elution was monitored at 220 nm. Fractions were collected, analyzed by LC-MS, and evaporated to dryness in a Speed Vac concentrator (Savant, Thermo Fisher Scientific, Waltham, MA, USA), resuspended in 10 mM ammonium bicarbonate, pH 8.0, digested with trypsin at 37 °C, enzyme-to-substrate ratio of 1 : 50 (w/w), overnight, and subjected to LC-MS/MS analysis.

Mass spectrometry and database search

LC-MS analysis was carried out on a ZQ system equipped with a Z-SPRAY source and a quadrupole analyzer, coupled to a 2690 Alliance HPLC using a Vydac C4 column (Waters-Micromass). The protein was eluted at a flow rate of 0.5 $mL\cdot min^{-1}$ with a 10–60% CH_3CN gradient in 0.1% TFA for 1 min. Data were elaborated using the MASSLYNX program (Waters-Micromass).

LC-MS/MS analyses were carried out on a CHIP MS 6520 QTOF equipped with a capillary 1200 HPLC system and a chip cube (Agilent Tech., Palo Alto, CA, USA). After loading, the peptide mixture (8 μL in 0.1% formic acid) was

first concentrated and washed at 4 μL·min^{-1} in a 40-nL enrichment column (Agilent Tech. chip), with 0.1% formic acid in 2% acetonitrile as eluent. The sample was then fractionated on a C18 reverse-phase capillary column (75 μm × 43 mm in the Agilent Tech. chip) at a flow rate of 400 nL·min^{-1}, with a linear gradient of eluent B (0.1% formic acid in 95% acetonitrile) in A (0.1% formic acid in 2% acetonitrile) from 7 to 60% for 50 min. Peptide analysis was performed using data-dependent acquisition of one MS scan (mass range from 400 to 2000 m/z) followed by MS/MS scans of the three most abundant ions in each MS scan.

Preliminarily, raw data from nano LC-MS/MS analyses were used to query nonredundant protein databases (UniprotSprot with taxonomy restriction to human), using in-house MASCOT software (Matrix Science, Boston, MA, USA) that established hDAAO and/or pLG72 as the principal components of the samples. These searches were performed with a parent mass tolerance of 20 p.p.m. and a fragment tolerance of 0.6 Da. Carbamidomethyl cysteine was searched as a constant modification. Variable modifications included methionine oxidation and peptide N-terminal glutamine cyclization to pyroglutamate. An average error of about 5 p.p.m. was observed for the experimental masses of linear peptides in respect to theoretical values.

Putative cross-linked peptides were identified with the open mass modification strategy developed by [30], using PROTEIN PROSPECTOR version 5.6. Open mass modification searches were performed against a restricted database consisting of hDAAO and pLG72 only. In such cases, mass modifications of any integer value between 138 (corresponding to intramolecular cross-linking) and 4000 Da on lysine, serine, and threonine residues or protein N termini were added to further modify the variables.

For the gel-free strategy, the MS/MS ion search of the human UniProt database by using the MASCOT software, with carboxyamidomethylation of cysteine as fixed modification and oxidation of methionine and pyro-Glu formation from Gln at the N terminus of peptides as the only variable modifications, assigned ions to linear peptides of both proteins and then used the results to prepare a list of signals the mass spectrometer should ignore for fragmentation in a subsequent run with the same sample. This procedure was used to search for species in low abundance such as those originating from cross-linked peptides. Raw data from the run with the exclusion list were analyzed according to the open mass modification strategy developed by [30] with Batch-Tag, MS-Bridge, and MS-Product tools within the PROTEIN PROSPECTOR package. All putative cross-links were then verified by manual inspection of the corresponding MS/MS spectrum.

Molecular modeling and design of pLG72 variants

The homology models of the pLG72 tertiary structure were built using the I-TASSER server [49] and the 3D structure of T4 lysozyme as template (pdb code 217l, overall sequence identity 20.8%). Model quality was evaluated using the Structure Analysis and Verification Server (SAVES, http://services.mbi.ucla.edu/SAVES/) and, in particular, taking into account results from the ERRAT algorithm [50]. A specific residue was considered belonging to the protein surface when its solvent-accessible surface was larger than 15 Å^2, as calculated using the PYMOL module findSurfaceResidues.

Molecular docking studies were performed by the AUTODOCK VINA, a package based on an iterated local search global algorithm [51]. The structure of the ligand CPZ was designed and energy-minimized using AVOGADRO [52], and the structure of pLG72 models produced by I-TASSER were used for docking simulations. PYMOL software was used to analyze docking results (www.pymol.org/).

Protein–protein docking simulations were performed using the ZDOCK server [53], the pLG72-VA model, and the experimental 3D structure of the hDAAO homodimer (pdb code 2e4a). Results were filtered such that only complexes having K62 (pLG72-VA) and T182 (hDAAO) in the interacting regions were returned from the server. Secondary structure composition was calculated with STRIDE [54].

Bioinformatics tools were used to design pLG72 variants; in particular, the secondary structure prediction server psipred (http://bioinf.cs.ucl.ac.uk/psipred/); the protein database BLASTP (http://blast.ncbi.nlm.nih.gov/blast/Blast); the Pfam protein families database (http://pfam.xfam.org/); and the MOBIDB 2.0, an improved database of intrinsically disordered and mobile proteins (http://mobidb.bio.unipd.it).

Analytical methods for protein characterization

hDAAO and pLG72 proteins were detected by western blot analysis using a rabbit anti-hDAAO polyclonal antibody (Davids Biotechnologie, Regensburg, Germany) or a rabbit anti-pLG72 polyclonal antibody (Santa Cruz Biotechnology Inc., Santa Cruz, CA, USA). A donkey anti-rabbit IgG antibody (Jackson ImmunoResearch, West Grove, PA, USA) was used as a secondary antibody coupled to the ECL system (GE Healthcare, Wauwatosa, WI, USA) for detection.

The oligomeric state of pLG72 proteins and interaction with hDAAO were determined by using a SEC-LS system consisting of a semipreparative size-exclusion chromatography column (Superdex200 10/30; GE Healthcare) by means of an Akta chromatographic system (GE Healthcare) coupled to a light-scattering detector (miniDAWN TREOS-Wyatt Technology Co., Santa Barbara, CA, USA) and a differential refractive index detector (Shodex RI-101). We collected, recorded, and processed the scattering data with the ASTRA software (5.3.4.14 version; Wyatt Technology). The following elution buffer was used: 20 mM Tris/HCl, pH 8.5, 150 mM sodium chloride, 5% glycerol, 5 mM 2-mercaptoethanol, 40 μM FAD, and 0.06% NLS.

Absorbance spectra were recorded at 25 °C using a Jasco 630 spectrophotometer (Jasco Europe, Cremella,

Italy): extinction coefficients at ~ 270 nm for the pLG72 variants were obtained by denaturing the protein variants in 20 mM Tris/HCl, pH 8.5, 100 mM NaCl, 5% glycerol, 5 mM 2-mercaptoethanol, 0.06% NLS, and 6 M urea, and using the theoretical extinction coefficients calculated with the protein parameter tool on the Expasy site (www.expasy.org).

Protein fluorescence spectra were recorded on a Jasco FP-750 spectrofluorimeter, using an excitation wavelength of 280 nm at a 0.5-μM protein concentration and at 15 °C. CD spectra were recorded on a Jasco J-715 or J-810 spectropolarimeter equipped with a Jasco PTC-343 Peltier thermostatic cell holder using a cell path length of 1 cm for measurements above 250 nm (0.4 mg protein·mL^{-1}) and 0.1 cm for measurements in the 190- to 260-nm range, at 20 °C [55]. Thermal denaturation analyses were conducted by following the CD signal at 265 nm by temperature ramp experiments in the 20–100 °C range; the sample was heated at a rate of 0.5 °C·min^{-1}. Spectra were recorded in 20 mM Tris/HCl pH 8.5, 150 mM NaCl, and 5% glycerol.

Surface plasmon resonance analysis

Real-time binding assays were performed on a Biacore 3000 surface plasmon resonance (SPR) instrument (GE Healthcare). Recombinant hDAAO (20 μg·mL^{-1}) was immobilized on a CM5 Biacore sensor chip (carboxymethylated dextran surface) (GE Healthcare) in 10 mM sodium acetate, pH 4.0, by using the EDC/NHS chemistry, to a final density of ~ 7000 resonance units; a flow cell with no immobilized protein was used as a control. Binding assays were carried out by injecting 60 μL of different concentrations of pLG72, pLG72$^{1–123}$, pLG72$^{1–94}$, pLG72$^{1–64}$, pLG72$^{72–153}$, and pLG72$^{122–153}$ at 20 μL·min^{-1}, using HBS-P20 (10 mM Hepes, pH 7.5, 0.1 M NaCl, 3 mM EDTA, and 0.005% P20; GE Healthcare) as running buffer. Each sensorgram was corrected for the response obtained in the control flow cell and normalized to baseline. BIAevaluation analysis package (version 4.1; GE Healthcare) was used to subtract the signal of the reference channel. As the rate of dissociation (k_{off}) is at the limit of the instrument record (< 1 E^{-6} s^{-1}), the affinity constant of the interaction was determined from the dependence of maximal intensity of the response on analyte concentrations (i.e., from the steady-state data and not from the kinetic ones). The fit of the equilibrium values for the SPR response (RU_{max} value) versus the ligand concentration was performed using the GRAPHPAD PRISM v4.00 (San Diego, CA, USA) and the one-site binding equation.

Acknowledgements

This work was supported by Fondo di Ateneo per la Ricerca to LP, SS, and GM.

Author contributions

SS and LPo conceived the project; GM performed the molecular modeling studies; SS, LC, PE, EP, and SDG performed biochemical studies, activity assays, and analyzed the data; EP and SDG designed the deletion variants; GS and LPi expressed, purified, and biochemically characterized the deleted variants; GS and LPi performed SPR analyses; LB and PP designed the cross-linking and limited proteolysis experiments and analyzed the data; IO and GL performed limited proteolysis and cross-linking experiments; LPo wrote the paper.

Conflict of interests

We declare no conflict of interests.

References

1 Pollegioni L, Piubelli L, Sacchi S, Pilone MS & Molla G (2007) Physiological functions of D-amino acid oxidases: from yeast to humans. *Cell Mol Life Sci* **64**, 1373–1394.
2 Sacchi S, Caldinelli L, Cappelletti P, Pollegioni L & Molla G (2012) Structure-function relationships in human D-amino acid oxidase. *Amino Acids* **43**, 1833–1850.
3 Pollegioni L & Sacchi S (2010) Metabolism of the neuromodulator D-serine. *Cell Mol Life Sci* **67**, 2387–2404.
4 Wolosker H & Mori H (2012) Serine racemase: an unconventional enzyme for an unconventional transmitter. *Amino Acids* **43**, 1895–1904.
5 Wolosker H (2011) Serine racemase and the serine shuttle between neurons and astrocytes. *Biochim Biophys Acta* **1814**, 1558–1566.
6 Machado-Vieira R, Manij HK & Zarate CA (2009) The role of the tripartite glutamatergic synapse in the pathophysiology and therapeutics of mood disorders. *Neuroscientist* **15**, 525–539.
7 Mundo E, Tharmalingham S, Neves-Pereira M, Dalton EJ, Macciardi F, Parikh SV, Bolonna A, Kerwin RW, Arranz MJ, Makoff AJ *et al.* (2003) Evidence that the N-methyl-D-aspartate subunit 1 receptor gene (GRIN1) confers susceptibility to bipolar disorder. *Mol Psychiatry* **8**, 241–245.
8 Sasabe J, Chiba T, Yamada M, Okamoto K, Nishimoto I, Matsuoka M & Aiso S (2007) D-serine is a key determinant of glutamate toxicity in amyotrophic lateral sclerosis. *EMBO J* **26**, 4149–4159.
9 Bagetta V, Ghiglieri V, Sgobio C, Calabresi P & Picconi B (2010) Synaptic dysfunction in Parkinson's disease. *Biochem Soc Trans* **38**, 493–497.
10 Demuro A, Parker I & Stutzmann GE (2010) Calcium signaling and amyloid toxicity in Alzheimer's disease. *J Biol Chem* **285**, 12463–12468.

11 Labrie V & Roder JC (2010) The involvement of the NMDA receptor D-serine/glycine site in the pathophysiology and treatment of schizophrenia. *Neurosci Biobehav Rev* **34**, 351–372.
12 Sacchi S, Bernasconi M, Martineau M, Mothet JP, Ruzzene M, Pilone MS, Pollegioni L & Molla G (2008) pLG72 modulates intracellular D-serine levels through its interaction with D-amino acid oxidase: effect on schizophrenia susceptibility. *J Biol Chem* **283**, 22244–22256.
13 Caldinelli L, Molla G, Bracci L, Lelli B, Pileri S, Cappelletti P, Sacchi S & Pollegioni L (2010) Effect of ligand binding on human D-amino acid oxidase: implications for the development of new drugs for schizophrenia treatment. *Protein Sci* **19**, 1500–1512.
14 Sacchi S, Cappelletti P, Giovannardi S & Pollegioni L (2011) Evidence for the interaction of D-amino acid oxidase with pLG72 in a glial cell line. *Mol Cell Neurosci* **48**, 20–28.
15 Cappelletti P, Campomenosi P, Pollegioni L & Sacchi S (2014) The degradation (by distinct pathways) of human D-amino acid oxidase and its interacting partner pLG72–two key proteins in D-serine catabolism in the brain. *FEBS J* **281**, 708–723.
16 Detera-Wadleigh SD & McMahon FJ (2006) G72/G30 in schizophrenia and bipolar disorder: review and meta-analysis. *Biol Psychiatry* **60**, 106–114.
17 Sacchi S, Binelli G & Pollegioni L (2016) *G72* primate-specific gene: a still enigmatic element in psychiatric disorders. *Cell Mol Life Sci* **73**, 2029–2039.
18 Verrall L, Burnet PW, Betts JF & Harrison PJ (2010) The neurobiology of D-amino acid oxidase and its involvement in schizophrenia. *Mol Psychiatry* **15**, 122–137.
19 Chumakov I, Blumenfeld M, Guerassimenko O, Cavarec L, Palicio M, Abderrahim H, Bougueleret L, Barry C, Tanaka H & La Rosa P *et al.* (2002) Genetic and physiological data implicating the new human gene G72 and the gene for D-amino acid oxidase in schizophrenia. *Proc Natl Acad Sci USA* **99**, 13675–13680.
20 Molla G, Bernasconi M, Sacchi S, Pilone MS & Pollegioni L (2006) Expression in Escherichia coli and in vitro refolding of the human protein pLG72. *Protein Expr Purif* **46**, 150–155.
21 Zappacosta F, Pessi A, Bianchi E, Venturini S, Sollazzo M, Tramontano A, Marino G & Pucci P (1996) Probing the tertiary structure of proteins by limited proteolysis and mass spectrometry: the case of Minibody. *Protein Sci* **5**, 802–813.
22 Scaloni A, Miraglia N, Orrù S, Amodeo P, Motta A, Marino G & Pucci P (1998) Topology of the calmodulin–melittin complex. *J Mol Biol* **277**, 945–958.
23 Casbarra A, Birolo L, Infusini G, Dal Piaz F, Svensson M, Pucci P, Svanborg C & Marino G (2004) Conformational analysis of HAMLET, the folding variant of human α-lactalbumin associated with apoptosis. *Protein Sci* **13**, 1322–1330.
24 Sinz A (2006) Chemical cross-linking and mass spectrometry to map three-dimensional protein structures and protein-protein interactions. *Mass Spectrom Rev* **25**, 663–682.
25 Sinz A (2014) The advancement of chemical cross-linking and mass spectrometry for structural proteomics: from single proteins to protein interaction networks. *Expert Rev Proteomics* **11**, 733–743.
26 Marino G, Pucci P, Birolo L & Ruoppolo M (2003) Exploitation of proteomic strategies in protein structure–function studies. *Pure Appl Chem* **75**, 303–310.
27 Kawazoe T, Tsuge H, Pilone MS & Fukui K (2006) Crystal structure of human D-amino acid oxidase: context-dependent variability of the backbone conformation of the VAAGL hydrophobic stretch located at the si-face of the flavin ring. *Protein Sci* **15**, 2708–2717.
28 Braun N, Zacharias M, Peschek J, Kastenmüller A, Zou J, Hanzlik M, Haslbeck M, Rappsilber J, Buchner J & Weinkauf J (2011) Multiple molecular architectures of the eye lens chaperone αB-crystallin elucidated by a triple hybrid approach. *Proc Natl Acad Sci USA* **108**, 20491–20496.
29 Mädler S1, Bich C, Touboul D & Zenobi R (2009) Chemical cross-linking with NHS esters: a systematic study on amino acid reactivities. *J Mass Spectrom* **44**, 694–706.
30 Chu F, Baker PR, Burlingame AL & Chalkley RJ (2010) Finding chimeras: a bioinformatics strategy for identification of cross-linked peptides. *Mol Cell Proteomics* **9**, 25–31.
31 Trnka MJ, Baker PR, Robinson PJ, Burlingame AL & Chalkley RJ (2014) Matching cross-linked peptide spectra: only as good as the worse identification. *Mol Cell Proteomics* **13**, 420–434.
32 Sehgal SA, Mannan S, Kanwal S, Naveed I & Mir A (2015) Adaptive evolution and elucidating the potential inhibitor against schizophrenia to target DAOA (G72) isoforms. *Drug Des Devel Ther* **9**, 3471–3480.
33 Sehgal SA, Khattak NA & Mir A (2013) Structural, phylogenetic and docking studies of D-amino acid oxidase activator (DAOA), a candidate schizophrenia gene. *Theor Biol Med Model* **10**, 3.
34 Merkley ED, Rysavy S, Kahraman A, Hafen RP, Daggett V & Adkins JN (2014) Distance restraints from crosslinking mass spectrometry: mining a molecular dynamics simulation database to evaluate lysine-lysine distances. *Protein Sci* **23**, 747–759.

35 Chang SLY, Hsieh C-H, Chen Y-J, Wang C-M, Shih C-S, Huang P-W, Mir A, Lane H-Y, Tsai GE & Chang H-T (2014) The C-terminal region of G72 increases D-amino acid oxidase activity. *Int J Mol Sci* **15**, 29–43.
36 Cheng L, Hattori E, Nakajima A, Woehrle NS, Opal MD, Zhang C, Grennan K, Dulawa SC, Tang YP, Gershon ES *et al.* (2014) Expression of the G72/G30 gene in transgenic mice induces behavioral changes. *Mol Psychiatry* **19**, 175–183.
37 Lewis DA & Levitt P (2002) Schizophrenia as a disorder of neurodevelopment. *Annu Rev Neurosci* **25**, 409–432.
38 Harrison PJ (1999) The neuropathology of schizophrenia. A critical review of the data and their interpretation. *Brain* **122**, 593–624.
39 Schumacher J, Jamra RA, Freudenberg J, Becker T, Ohlraun S, Otte AC, Tullius M, Kovalenko S, Bogaert AV, Maier W *et al.* (2004) Examination of G72 and D-amino-acid oxidase as genetic risk factors for schizophrenia and bipolar affective disorder. *Mol Psychiatry* **9**, 203–207.
40 Harrison PJ & Weinberger DR (2005) Schizophrenia genes, gene expression, and neuropathology: on the matter of their convergence. *Mol Psychiatry* **10**, 40–68.
41 Ross CA, Margolis RL, Reading SA, Pletnikov M & Coyle JT (2006) Neurobiology of schizophrenia. *Neuron* **52**, 139–153.
42 Papouin T, Ladépêche L, Ruel J, Sacchi S, Labasque M, Hanini M, Groc L, Pollegioni L, Mothet JP & Oliet SH (2012) Synaptic and extrasynaptic NMDA receptors are gated by different endogenous coagonists. *Cell* **150**, 633–646.
43 Kvajo M, Dhilla A, Swor DE, Karayiorgou M & Gogos JA (2008) Evidence implicating the candidate schizophrenia/bipolar disorder susceptibility gene G72 in mitochondrial function. *Mol Psychiatry* **13**, 685–696.
44 Terry-Lorenzo RT, Masuda K, Sugao K, Fang QK, Orsini MA, Sacchi S & Pollegioni L (2015) High-throughput screening strategy identifies allosteric, covalent human D-amino acid oxidase inhibitor. *J Biomol Screen* **20**, 1218–1231.
45 Krissinel E & Henrick K (2007) Inference of macromolecular assemblies from crystalline state. *J Mol Biol* **372**, 774–797.
46 Habchi J, Tompa P, Longhi S & Uversky VN (2014) Introducing protein intrinsic disorder. *Chem Rev* **114**, 6561–6588.
47 Tompa P, Schad E, Tantos A & Kalmar L (2015) Intrinsically disordered proteins: emerging interaction specialists. *Curr Opin Struct Biol* **35**, 49–59.
48 Molla G, Sacchi S, Bernasconi M, Pilone MS, Fukui K & Pollegioni L (2006) Characterization of human D-amino acid oxidase. *FEBS Lett* **580**, 2358–2364.
49 Roy A, Kucukural A & Zhang Y (2010) I-TASSER: a unified platform for automated protein structure and function prediction. *Nat Protoc* **5**, 725–738.
50 Colovos C & Yeates TO (1993) Verification of protein structures: patterns of nonbonded atomic interactions. *Protein Sci* **2**, 1511–1519.
51 Trott O & Olson AJ (2010) AutoDock Vina: improving the speed and accuracy of docking with a new scoring function, efficient optimization, and multithreading. *J Comput Chem* **31**, 455–461.
52 Hanwell MD, Curtis DE, Lonie DC, Vandermeersch T, Zurek E & Hutchison GR (2012) Avogadro: an advanced semantic chemical editor, visualization, and analysis platform. *J Cheminform* **4**, 17.
53 Pierce BG, Hourai Y & Weng Z (2011) Accelerating protein docking in ZDOCK using an advanced 3D convolution library. *PLoS One* **6**, e24657.
54 Frishman D & Argos P (1995) Knowledge-based protein secondary structure assignment. *Proteins* **23**, 566–579.
55 Caldinelli L, Iametti S, Barbiroli A, Bonomi F, Piubelli L, Ferranti P, Picariello G, Pilone MS & Pollegioni L (2004) Unfolding intermediate in the peroxisomal flavoprotein D-amino acid oxidase. *J Biol Chem* **279**, 28426–28434.